Received July 26, 2019, accepted August 5, 2019, date of publication August 9, 2019, date of current version August 29, 2019.

Digital Object Identifier 10.1109/ACCESS.2019.2934187

Integration of Numerical Simulation and Control Scheme for Energy Conservation of Aluminum Melting Furnaces

NA GUO[1], HONGYU ZHENG[2], TAO ZOU[3,4], AND YANG JIA[3,4]

[1]College of Engineering, Shenyang Agricultural University, Shenyang 110866, China
[2]School of Intelligent Manufacturing, Huanghuai University, Zhumadian 463000, China
[3]Shenyang Institute of Automation, Chinese Academy of Sciences, Shenyang 110016, China
[4]Institutes for Robotics and Intelligent Manufacturing, Chinese Academy of Sciences, Shenyang 110016, China

Corresponding authors: Hongyu Zheng (zhenghongyu@sia.cn) and Tao Zou (zoutao@sia.cn)

This work was supported in part by the National Key Research and Development Program of China under Grant 2017YFA0700303, in part by the National Natural Science Foundation of China under Grant 61773366, and in part by the Ph.D. Start-up Fund of Liaoning Province under Grant 20180540066.

ABSTRACT Aluminum melting process is a semi-continuous process with high-energy consumption. In this paper, a software-based strategy which considers numerical simulation and control scheme simultaneously is employed to improve energy consumption of aluminum melting furnaces without changing the hardware. For numerical simulation, a nonlinear steady-state optimization is performed offline to obtain optimal operating points. Extensively, the optimal operating conditions include not only product exit temperature, but also ratio of combustion air flow and natural gas flow, furnace temperature, flue gas temperature and some important manipulated variables. For control scheme, a two-layer model predictive control which consists of steady state target calculation and dynamic optimization is developed to track the optimal operating conditions. In steady state target calculation layer, a priority strategy is proposed based on the different importance of controlled variables to make the steady state targets more reasonably. In dynamic optimization layer, a quadratic objective function is defined in terms of tracking both the optimal steady-state of controlled variables and manipulated variables. The method is successfully carried out in F1 aluminum melting furnace of a company in Tianjin. Compared with previous operation, the comprehensive energy consumption and the comprehensive energy consumption for unit output of product decrease 5.99% and 6.56% respectively.

INDEX TERMS Melting processing, predictive control, control engineering, steady-state target calculation.

I. INTRODUCTION

Aluminum and aluminum alloy products, which have good mechanical property and superb cast ability, are widely used in automobile, construction, communication and other fields [1]. Aluminum melting alone contributes more than 50% of a plant's total energy consumption, along with massive CO2 emissions and other waste production [1], [2]. In view of huge energy-cost and increasingly stringent emissions regulations, much attention has been paid to research and applications on energy conservation and emissions reduction for melting furnace [3]. There are two main melting furnace types: electric and fuel-fired. The energy conservation technology for melting furnaces can be classified into hardware-based strategy and software-based strategy. This paper is focused on software-based strategy for fuel-fired aluminum melting furnaces.

Subject to existing hardware, the software-based strategies of reducing energy consumption have been reviewed in the literature [4]–[7]. There are many studies focusing on numerical simulation, e.g., [2], [8], [9]. In the literature [9], CFD technique combining with Taguchi method and cross-table-based analysis of variance was developed to optimize the parameter of melting process of an aluminum melting furnace. The optimal conditions of horizontal angle between burners, air preheated temperature, natural gas mass flow and air-fuel ratio were determined. However, the results of these numerical simulations are usually used to guide the operation offline for the high computation complexity.

Additionally, several control schemes have been developed. Classical Proportional-Integral-Derivative (PID) is the most common industrial controller [10]. To maintain

The associate editor coordinating the review of this article and approving it for publication was Nishant Unnikrishnan.

the furnace temperature of a melting process with large time delay at a setpoint, smith predictor and other advanced algorithms combining with smith predictor which are used to compensate large time delay were proposed [11], [12]. To maintain the effective product exit temperature, Beschi *et al.* [13] presented a PI controller with model-based feedforward considering process input constraints. The optimal feedforward control law is addressed by employing an input-output inversion of the system.

Rule-based controllers which operate on a set of rules defined prior to actual operation are frequently used [14]. Martín *et al.* [15] proposed a fuzzy system of Takagi–Sugeno–Kang. The system was used to obtain the IF–THEN rules where the THEN parts are linear combinations of input variables. Based on these IF–THEN rules, the control actions are evaluated, and carried out to maintain the product exit temperature at a set point. To minimize the electricity consumption of a magnesium furnaces, a class of stable control rules with respect to the current values were proposed to heat the product up to an appropriate temperature zone [16]. However, for the rules based on massive expert knowledge and the complexity of the melting process, the rule-based controllers are expensive to install, commission and tune.

Model predictive control (MPC), which can easily and effectively deal with of multivariable systems with interactions and constraints, has been widely adopted in industry [17], [18]. In order to track the optimal air factor, Grancharova *et al.* [19] proposed an explicit reference tracking NMPC controller for a combustion plant. The NMPC controller which is based on a Gaussian process model takes the economic and the environment into account simultaneously, and simulation showed that the optimal operation of the combustion plant is achieved. However, considering the operation safety of the combustion plant and the disallowed interrupts in plant operation, the explicit stochastic NMPC has not be implemented in practical application. Zhang *et al.* presented an enhanced MPC based on a first-order plus dead time (FOPDT) model to control the furnace temperature of a heating furnace [20]. Ganesh *et al.* developed a two-layer hierarchical structure which consists of a regulatory controller and a MPC controller to control the product exit temperature for an austenitization furnace [21]. Banerjee *et al.* [22] presented a model-based control method to simultaneously reduce the energy consumption and minimize the deviations of the product exit temperature from prescribed values. For combustion optimization, an advanced combustion controller based on model-based predictive control technology [23] was proposed to keep the pressure under limit with simultaneous air-fuel ratio optimization, and is deployed in this paper.

From the above we can see that there are many studies in the literature focusing on the software-based strategy of fuel-fired melting furnaces from the view of numerical simulation and control scheme. To achieve higher performance, it is important that numerical simulation and control scheme are designed together. However, there are few researches treating both aspects in fuel-fired melting furnaces. In this paper, a software-based strategy which considers numerical simulation and control scheme simultaneously is employed to improve energy consumption. To overcome the problem of high computational cost of numerical simulation, a nonlinear steady-state model of the melting furnace is adopted to obtain the optimal operating conditions offline. Extensively, the optimal operating conditions include not only product exit temperature, but also ratio of combustion air flow and natural gas flow, furnace temperature, flue gas temperature and some important manipulated variables. A two-layer MPC which consists of steady state target calculation (SSTC) and dynamic optimization (DO), different form that in [21], is developed to track the optimal operating conditions. Owing to the different importance of controlled variables, a priority strategy is considered in SSTC layer to make the steady state targets more suitable. The steady state targets calculated by SSTC are tracked in DO layer. To settle the problem of serious interactions and large disturbances, a partially decentralized model is adopted in DO to improve robustness. An application of this method on F1 aluminum melting furnace in Tianjin, China is successfully carried out.

The paper is organized as follows. Firstly, a fuel-fired aluminum melting furnace with two chambers is described, next the energy conservation oriented multivariable two-layer MPC method is illustrated in detail, and then an offline numerical simulation and controller design of F1 aluminum melting furnace is introduced, and the performance before and after the application of the controller is contrasted and analyzed, the research is summarized in the last.

II. FUEL-FIRED ALUMINUM MELTING FURNACE

A representative schematic of fuel-fired aluminum melting furnace used widely is presented in Figure 1. The furnace has two molten pools, a main molten pool and an auxiliary molten pool. Liquid aluminum in the two molten pools is circulated through a circulating pump. The primary heat for smelting aluminum in the main molten pool is gained from burned natural gas, and in the auxiliary molten pool is gained from circulating liquid aluminum and flue gas. There are three feeding methods: 1) large-block aluminums are charged intermittently through the main/auxiliary furnace door; 2) aluminum debris are feed continuously through 1# rotary kiln; 3) aluminum scraps are add continuously through 2# rotary kiln. When the level and quality of liquid aluminum meet requirements after drossing and sample analysis, part of liquid aluminum is transferred to next production sections as required.

The flue gas partially passes through 1# and 2# rotary kiln to heat up the raw material of solid aluminum for improving the residual heat utilization, then though a bag-type dust remover and an induced draft fan, and finally is discharged though a chimney.

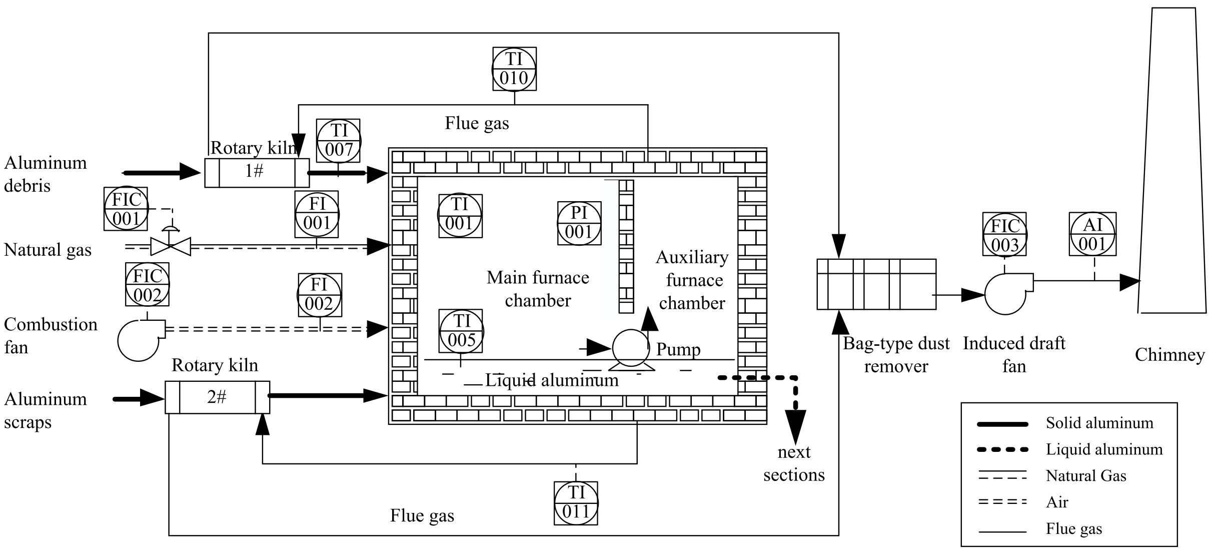

FIGURE 1. Diagram of fuel-fired aluminum melting furnace.

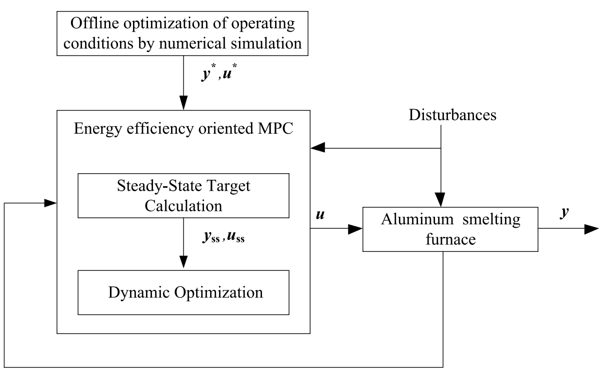

FIGURE 2. Structure of energy conservation oriented two-layer MPC.

III. ENERGY CONSERVATION ORIENTED TWO-LAYER MPC FOR MELTING PROCESS

Even though the aluminum melting process described in Figure 1 is a semi-continuous process, for the convenience of calculation, we assume that the melting process is a continuous process and the intermittent charging is a disturbance. Using the experience of hierarchical control architectures in continuous process industry for reference, an energy conservation oriented multi-variable two-layer MPC for aluminum melting furnace focusing on the multi-target optimization is presented. The structure is shown in Figure 2. Where $\boldsymbol{u} \in \mathbb{R}^{nu}$ is the vector of manipulated variables including the openness of the natural gas valve, the frequency of the combustion air fan and the frequency of the induced draft fan; $\boldsymbol{y} \in \mathbb{R}^{ny}$ is the vector of controlled variables including the furnace chamber temperature, the liquid aluminum temperature, the flue gas temperature, the aluminum scraps temperature, the oxygen content in the flue gas and the furnace pressure. An offline nonlinear steady-state optimization executed at the beginning of design instead of the real-time optimization (RTO) for convenience. The optimal operating points $(\boldsymbol{u}^*, \boldsymbol{y}^*)$ are calculated by offline optimization are transmitted to SSTC, the upper layer of two-layer MPC. The lower layer DO receive the optimal steady-state targets $(\boldsymbol{u}_{SS}, \boldsymbol{y}_{SS})$ from SSTC as the set-points for the MPC for implementation.

A. OFFLINE OPTIMIZATION OF OPERATING CONDITONS BY NUMERICAL SIMULATION

A comprehensive energy consumption for unit output of product is defined as energy conservation evaluation index.

$$e_p = \frac{E}{P} \tag{1}$$

where e_p is the comprehensive energy consumption for unit output of product; E is comprehensive energy consumption, including the heat energy released by fuel combustion and the electrical energy consumed by fans; P is the total output of acceptable liquid aluminum.

From (1), the reduction of the total amount of consumed energy and decreasing the burn loss are effective measures of energy conservation. Considering the following direct measures and indirect measures comprehensively:

1) Maintaining the optimal ratio of combustion air flow and natural gas flow to minimize excess oxygen.
2) Minimizing the flue gas temperature.
3) Maintaining the furnace temperature at an optimal value.
4) Minimizing the effective product exit temperature.
5) Minimizing burning loss of material.

An offline nonlinear steady-state optimization is performed to provide the optimal operating points to two-layer MPC. The major cost for melting process is fuel, electricity and burning loss. Therefore, the optimization problem can be described below:

$$\begin{aligned}&\min_{\boldsymbol{u},\boldsymbol{y}}\ C_1F_{\mathrm{NG}}+C_2F_{\mathrm{CA}}+C_3F_{\mathrm{IA}}+C_4F_{\mathrm{BL}}\\&s.t.\,f\left(\boldsymbol{u},\boldsymbol{y}\right)=0\\&\quad g\left(\boldsymbol{u},\boldsymbol{y}\right)\le 0,\end{aligned}\tag{2}$$

where F_{NG}, F_{CA}, F_{IA} and F_{BL} denote natural gas flow, power consumption of combustion air fan, power consumption of induced draft fan and burning loss flow respectively; C_1, C_2, C_3 and C_4 are their cost coefficients; f is the first principle model of melting process; g is the process constraints, such as production safety and product quality limits. Then the optimal operating points ($\boldsymbol{u}^*, \boldsymbol{y}^*$) are obtained by solving the nonlinear optimization problem offline.

B. ENERGY CONSERVATION ORIENTED TWO-LAYER MPC

Due to the presence of unmeasured disturbances and operating conditions change, the optimal operating points ($\boldsymbol{u}^*, \boldsymbol{y}^*$) obtained from the nonlinear model may not be fixed all the time. On the other hand, the nonlinear steady-state model used in nonlinear steady-state optimization may not be consistent with the linear model used in MPC, which implies that MPC may not be guaranteed to drive the process variables ($\boldsymbol{u}, \boldsymbol{y}$) to their optimal operating points ($\boldsymbol{u}^*, \boldsymbol{y}^*$). Therefore, a two-layer MPC consisting of SSTC in the upper layer and DO in the lower layer is introduced [17].

1) MULTIPRIORITY-BASED STEADY-STATE TARGET CALCULATION

The SSTC objective function for aluminum melting process are mathematically formulated as

$$\ell_e(k) \triangleq \boldsymbol{W}_e^T \boldsymbol{u}_{\mathrm{SS}}\left(k\right) \tag{3a}$$

$$\ell_t(k) \triangleq \left[\boldsymbol{y}^* - \boldsymbol{y}_{\mathrm{SS}}\left(k\right)\right]^T \boldsymbol{W}_t[\boldsymbol{y}^* - \boldsymbol{y}_{\mathrm{SS}}\left(k\right)] \tag{3b}$$

$$\ell_\Delta(k) \triangleq \Delta\boldsymbol{u}_{\mathrm{SS}}^T\left(k\right)\boldsymbol{W}_\Delta \Delta\boldsymbol{u}_{\mathrm{SS}}\left(k\right) \tag{3c}$$

$$\ell_s\left(k\right) \triangleq \boldsymbol{\varepsilon}_{\mathrm{SS}}^T\left(k\right)\boldsymbol{W}_s\boldsymbol{\varepsilon}_{\mathrm{SS}}\left(k\right) \tag{3d}$$

where $\boldsymbol{u}_{\mathrm{SS}}\left(k\right)$ and $\boldsymbol{y}_{\mathrm{SS}}\left(k\right)$ are the steady-state inputs and outputs at time k respectively; $\ell_e \in \mathbb{R}_{\ge 0}$ denotes the economic cost of aluminum melting process operation, such as cost of fuel (natural gas) and cost of electricity (induced draft fan and combustion air fan). The cost $\ell_t \in \mathbb{R}_{\ge 0}$ penalizes steady-state output deviations from the optimal operating condition $\boldsymbol{y}^*$, for instance, the nearer air-fuel ratio approximates to its optimal value calculated by nonlinear optimization, the better combustion efficiency is. The cost $\ell_\Delta(k) \in \mathbb{R}_{\ge 0}$ penalizes the steady-state input variations $\Delta\boldsymbol{u}_{\mathrm{SS}}\left(k\right) = \boldsymbol{u}_{\mathrm{SS}}\left(k\right) - \boldsymbol{u}(k-1)$ to gain a smooth operation and extending components life. $\ell_s(k)$ represents the penalization of constraint violations, and $\boldsymbol{\varepsilon}_{\mathrm{SS}}\left(k\right)$ is slack variable to guarantee the feasibility of the optimization problem. $\boldsymbol{W}_e$ is a vector which is determined by the comprehensive benefit or cost of steady-state inputs and outputs variable on a same measurement scale; $\boldsymbol{W}_t$, $\boldsymbol{W}_\Delta$ and $\boldsymbol{W}_s$ are diagonal positive definitive matrices of appropriate dimensions. $\boldsymbol{W}_t$ and $\boldsymbol{W}_s$ yield more control efforts to achieve tighter control of more important controlled outputs, and $\boldsymbol{W}_\Delta$ directs a more robust controller but at the cost of the controller being more sluggish.

According to the objectives in (3), the SSTC optimization problem of aluminum melting process can be formulated as

$$\min_{\boldsymbol{u}_{\mathrm{SS}},\boldsymbol{y}_{\mathrm{SS}},\boldsymbol{\varepsilon}}\ \ell_e\left(k\right)+\ell_t\left(k\right)+\ell_\Delta\left(k\right)+\ell_s(k) \tag{4a}$$

$$\text{s.t. } \boldsymbol{y}_{\mathrm{SS}}(k+1) = \boldsymbol{G}_0\Delta\boldsymbol{u}_{\mathrm{SS}}(k) + \tilde{\boldsymbol{y}}\left(k+N|k\right) \tag{4b}$$

$$\boldsymbol{y}_{\mathrm{LL}} - \boldsymbol{\varepsilon}_{\mathrm{SS}}(k) \le \boldsymbol{y}_{\mathrm{SS}}(k+1) \le \boldsymbol{y}_{\mathrm{HL}} + \boldsymbol{\varepsilon}_{\mathrm{SS}}(k) \tag{4c}$$

$$\boldsymbol{u}_{\mathrm{LL}} \le \boldsymbol{u}_{\mathrm{SS}}(k) \le \boldsymbol{u}_{\mathrm{HL}} \tag{4d}$$

$$-\boldsymbol{\varepsilon}_{\mathrm{SS}}(k) \le \boldsymbol{0} \tag{4e}$$

where (4b) is the steady-state model of process; $\boldsymbol{G}_0$ is the steady-state gain matrix. $\tilde{\boldsymbol{y}}\left(k+N|k\right)$ is the open loop prediction of controlled variables at time $k+N$ computed at time k, and N is the settling time of aluminum melting process. $\boldsymbol{y}_{\mathrm{LL}}$ and $\boldsymbol{y}_{\mathrm{HL}}$ are minimum and maximum bounds of the controlled variables, $\boldsymbol{u}_{\mathrm{LL}}$ and $\boldsymbol{u}_{\mathrm{HL}}$ are the bounds of the manipulated variables. The optimal steady-state targets ($\boldsymbol{u}_{\mathrm{SS}}^*, \boldsymbol{y}_{\mathrm{SS}}^*$) will be obtained using quadratic programming, (5) describes the standard quadratic program (QP) form of (4).

$$\begin{aligned}&\min_{\boldsymbol{Z}}\ \boldsymbol{Z}^T\boldsymbol{W}\boldsymbol{Z}+\boldsymbol{H}^T\boldsymbol{Z}\\&s.t.\,\boldsymbol{\theta}\boldsymbol{Z}\le\boldsymbol{b}\end{aligned}\tag{5}$$

where,

$$\boldsymbol{Z}=\begin{bmatrix}\Delta\boldsymbol{u}_{\mathrm{SS}}(k)\\ \boldsymbol{\varepsilon}_{\mathrm{SS}}(k)\end{bmatrix},$$

$$\boldsymbol{W}=\begin{bmatrix}\boldsymbol{G}_0^T\boldsymbol{W}_t\boldsymbol{G}_0+\boldsymbol{W}_\Delta & \boldsymbol{0}\\ \boldsymbol{0} & \boldsymbol{W}_s\end{bmatrix},$$

$$\mathbf{H}=\begin{bmatrix}\boldsymbol{W}_e-2(\boldsymbol{y}^*-\tilde{\boldsymbol{y}}\left(k+N|k\right))\boldsymbol{W}_t\boldsymbol{G}_0\\ \boldsymbol{0}\end{bmatrix},$$

$$\boldsymbol{\theta}=\begin{bmatrix}\boldsymbol{G}_0 & -\boldsymbol{I}\\ -\boldsymbol{G}_0 & -\boldsymbol{I}\\ \boldsymbol{I} & \boldsymbol{0}\\ -\boldsymbol{I} & \boldsymbol{0}\\ \boldsymbol{0} & -\boldsymbol{I}\end{bmatrix},\boldsymbol{b}=\begin{bmatrix}\boldsymbol{y}_{\mathrm{HL}}-\tilde{\boldsymbol{y}}\left(k+N|k\right)\\ -\boldsymbol{y}_{\mathrm{LL}}+\tilde{\boldsymbol{y}}\left(k+N|k\right)\\ \boldsymbol{u}_{\mathrm{HL}}-\boldsymbol{u}(k-1)\\ -\boldsymbol{u}_{\mathrm{LL}}+\boldsymbol{u}\left(k-1\right)\\ \boldsymbol{0}\end{bmatrix}.$$

In SSTC, the importance of constraints of different variables varies, and it is unreasonable to relax constraints irregularly in order to obtain feasible solutions. To settle this problem, this paper presents a multipriority-based SSTC method which sorts the priority order of controlled variables according to importance, such as production safety, product quality and economic benefit, then constraints are relaxed.

a: FEASIBILITY JUDGMENT

Here the feasibility is obtained by minimizing a positive definite quadratic cost function

$$\min_{\boldsymbol{Z}} J = \boldsymbol{\varepsilon}_{\mathrm{SS}}^T\left(k\right)\boldsymbol{W}_f\boldsymbol{\varepsilon}_{\mathrm{SS}}\left(k\right) \tag{6}$$

Constrains are the same as (5), and not repeated here. $\boldsymbol{W}_f$ is a diagonal positive definite matrix. For the optimization solution J^* of (6), one may in general discern the following two cases.

$J^* = 0$: it means that the constraint set of (5) is not null in the absence of relaxation conditions, and there is a feasible solution which can be directly calculated by (5).

$J^* \neq 0$: it means that the constraint set of (5) is null in the absence of relaxation conditions. Therefore, constraints relaxation is required for SSTC.

b: CONSTRAINTS RELAXATION BASED ON PRIORITY

Suppose that the controlled variables have p different priorities, which are denoted as $P^1, P^2, \cdots, P^p$ from low to high respectively, where the lower the numerical value, the higher the priority.

We first relax the controlled variable constraints with the highest priority (P^1), considering the optimization problem where only the controlled variables with P^1 priority is considered.

$$\begin{aligned} &\min_{\boldsymbol{Z}^1} \ J^1 = \boldsymbol{Z}^{1T}\boldsymbol{W}_f^1\boldsymbol{Z}^1 \\ &s.t.\ \boldsymbol{\theta}^1\boldsymbol{Z}^1 \leq \boldsymbol{b}^1 \end{aligned} \tag{7}$$

where,

$$\boldsymbol{Z}^1 = \begin{bmatrix} \Delta\boldsymbol{u}_{\mathrm{SS}}(k) \\ \boldsymbol{\varepsilon}_{\mathrm{SS}}^1(k) \end{bmatrix}_{(nu+n1)\times 1},$$

$$\boldsymbol{\theta}^1 = \begin{bmatrix} \boldsymbol{G}_0^1 & -\boldsymbol{I}^1 \\ -\boldsymbol{G}_0^1 & -\boldsymbol{I}^1 \\ \boldsymbol{I} & \boldsymbol{0}^1 \\ -\boldsymbol{I} & \boldsymbol{0}^1 \\ \boldsymbol{0} & -\boldsymbol{I}^1 \end{bmatrix}_{(3n1+2nu)\times(nu+n1)},$$

and

$$\boldsymbol{b}^1 = \begin{bmatrix} \boldsymbol{y}_{\mathrm{HL}}^1 - \tilde{\boldsymbol{y}}^1(k+N|k) \\ -\boldsymbol{y}_{\mathrm{LL}}^1 + \tilde{\boldsymbol{y}}^1(k+N|k) \\ \boldsymbol{u}_{\mathrm{HL}} - \boldsymbol{u}(k-1) \\ -\boldsymbol{u}_{\mathrm{LL}} + \boldsymbol{u}(k-1) \\ \boldsymbol{0} \end{bmatrix}_{(3n1+2nu)\times 1}.$$

The superscript number refers to priority. $\boldsymbol{\varepsilon}_{\mathrm{SS}}^1(k)$ indicates the slack variable with P^1 priority, and so on. $n1$ is the number of controlled variables with P^1 priority. $\boldsymbol{W}_f^1$ is a weighting matrix. The optimal solution for $\boldsymbol{\varepsilon}_{\mathrm{SS}}^1(k)$ is denoted as $\boldsymbol{\varepsilon}_{\mathrm{SS}}^{1*}(k)$. The constraint relaxation of P^1 priority is determined at this point, then we move to the next priority (P^2) optimization problem.

$$\begin{aligned} &\min_{\boldsymbol{Z}^2} \ J^2 = \boldsymbol{Z}^{2T}\boldsymbol{W}_f^2\boldsymbol{Z}^2 \\ &s.t.\ \boldsymbol{\theta}^2\boldsymbol{Z}^2 \leq \boldsymbol{b}^2 \end{aligned} \tag{8}$$

where

$$\boldsymbol{Z}^2 = \begin{bmatrix} \Delta\boldsymbol{u}_{\mathrm{SS}}(k) \\ \boldsymbol{\varepsilon}_{\mathrm{SS}}^2(k) \end{bmatrix}_{(nu+n2)\times 1},$$

$$\boldsymbol{\theta}^2 = \begin{bmatrix} \boldsymbol{G}_0^1 & \boldsymbol{0}^1 \\ \boldsymbol{G}_0^2 & -\boldsymbol{I}^2 \\ -\boldsymbol{G}_0^1 & \boldsymbol{0}^1 \\ -\boldsymbol{G}_0^2 & -\boldsymbol{I}^2 \\ \boldsymbol{I} & \boldsymbol{0}^2 \\ -\boldsymbol{I} & \boldsymbol{0}^2 \\ \boldsymbol{0} & -\boldsymbol{I}^2 \end{bmatrix}_{(2n1+3n2+2nu)\times(nu+n2)},$$

and

$$\boldsymbol{b}^2 = \begin{bmatrix} \boldsymbol{y}_{\mathrm{HL}}^1 - \tilde{\boldsymbol{y}}^1(k+N|k) + \boldsymbol{\varepsilon}_{\mathrm{SS}}^{1*}(k) \\ \boldsymbol{y}_{\mathrm{HL}}^2 - \tilde{\boldsymbol{y}}^2(k+N|k) \\ -\boldsymbol{y}_{\mathrm{LL}}^1 + \tilde{\boldsymbol{y}}^1(k+N|k) + \boldsymbol{\varepsilon}_{\mathrm{SS}}^{1*}(k) \\ -\boldsymbol{y}_{\mathrm{LL}}^2 + \tilde{\boldsymbol{y}}^2(k+N|k) \\ \boldsymbol{u}_{\mathrm{HL}} - \boldsymbol{u}(k-1) \\ -\boldsymbol{u}_{\mathrm{LL}} + \boldsymbol{u}(k-1) \\ \boldsymbol{0} \end{bmatrix}_{(2n1+3n2+2nu)\times 1}.$$

It is important to note that the slack variable $\boldsymbol{\varepsilon}_{\mathrm{SS}}^1(k)$ is determined in the optimization of constraints relaxation with last priority, therefore the solution $\boldsymbol{\varepsilon}_{\mathrm{SS}}^{1*}(k)$ is treated as a known value instead of a decision variable. According to the optimization problem (8), the optimal relaxation $\boldsymbol{\varepsilon}_{\mathrm{SS}}^{2*}(k)$ can be obtained. In the same way, we can generalize other optimal relaxations $\boldsymbol{\varepsilon}_{\mathrm{SS}}^{3*}(k), \cdots, \boldsymbol{\varepsilon}_{\mathrm{SS}}^{p*}(k)$.

Finally, the optimal steady-state inputs $\boldsymbol{u}_{\mathrm{SS}}^*(k)$ and outputs $\boldsymbol{y}_{\mathrm{SS}}^*(k)$ can be obtained by substituting $\boldsymbol{\varepsilon}_{\mathrm{SS}}^*(k)$ into (5). Here $\boldsymbol{\varepsilon}_{\mathrm{SS}}^*(k) = \left[\boldsymbol{\varepsilon}_{\mathrm{SS}}^{1*T}(k) \cdots \boldsymbol{\varepsilon}_{\mathrm{SS}}^{p*T}(k)\right]^T$.

2) DYNAMIC OPTIMIZATION

The lower layer DO implements MPC to regulate the inputs and outputs to their optimal steady-state targets from the upper layer SSTC.

Here, a step response model obtained easily in industry for MPC is used to describe the melting process. Suppose that the step responses coefficient of output variable y_i for input variable u_j is $\boldsymbol{g}_{ij} = \left[g_{ij}(1), \cdots, g_{ij}(N)\right]^T$, where $i = 1, \cdots, ny$, $j = 1, \cdots, nu$. N is the model length. Define vectors as follows:

$$\begin{aligned} \tilde{\boldsymbol{y}}_{P0}(k) &= [\tilde{\boldsymbol{y}}_0(k+1|k), \cdots, \tilde{\boldsymbol{y}}_0(k+P|k)] \\ \tilde{\boldsymbol{y}}_{PM}(k) &= [\tilde{\boldsymbol{y}}(k+1|k), \cdots, \tilde{\boldsymbol{y}}(k+P|k)] \\ \Delta\boldsymbol{u}_M(k) &= [\Delta\boldsymbol{u}(k), \cdots, \Delta\boldsymbol{u}(k+M-1)] \\ \boldsymbol{G}_{ij} &= \begin{bmatrix} g_{ij}(1) & \cdots & 0 \\ \vdots & \ddots & \vdots \\ g_{ij}(M) & \cdots & g_{ij}(1) \\ \vdots & \vdots & \vdots \\ g_{ij}(P) & \cdots & g_{ij}(P-M+1) \end{bmatrix} \\ \boldsymbol{G} &= \begin{bmatrix} \boldsymbol{G}_{11} & \boldsymbol{G}_{12} & \cdots & \boldsymbol{G}_{1nu} \\ \boldsymbol{G}_{21} & \boldsymbol{G}_{22} & \cdots & \boldsymbol{G}_{2nu} \\ \vdots & \vdots & & \vdots \\ \boldsymbol{G}_{ny1} & \boldsymbol{G}_{ny2} & \cdots & \boldsymbol{G}_{nynu} \end{bmatrix} \end{aligned}$$

where P and M denote prediction horizon and control horizon, respectively; $\tilde{\boldsymbol{y}}_{P0}(k)$ is the initial output prediction value of the melting process at time k; $\tilde{\boldsymbol{y}}_{PM}(k)$ is the future output prediction value over the prediction horizon P at time k after adding M control movements $\Delta\boldsymbol{u}_M(k)$; $\boldsymbol{G}$ is the dynamic gain matrix. it notes that the inputs are assumed to be constant after time $k+M$, i.e. $\Delta\boldsymbol{u}(k+M+i)=0$, for $i=1,\cdots,P-1$. Hence, the step response model with multi-step prediction for the melting process can be written as:

$$\tilde{\boldsymbol{y}}(k+1)=\tilde{\boldsymbol{y}}_0(k+1)+\boldsymbol{G}\Delta\boldsymbol{u}_M(k) \tag{9}$$

A standard MPC is described as minimizing the following dynamic objective function to drive outputs to their setpoints $\boldsymbol{y}_{SP}$.

$$\min_{\substack{\Delta\boldsymbol{u}(k),\cdots,\Delta\boldsymbol{u}(k+M-1)\\ \boldsymbol{\varepsilon}(k),\cdots,\boldsymbol{\varepsilon}(k)}} \sum_{i=1}^{P}\left\|\boldsymbol{y}_{SP}(k)-\tilde{\boldsymbol{y}}(k+i)\right\|_{\boldsymbol{Q}_i}^2 + \sum_{i=1}^{M}\|\Delta\boldsymbol{u}(k+i)\|_{\boldsymbol{R}_i}^2 + \sum_{i=1}^{P}\|\boldsymbol{\varepsilon}(k+i)\|_{\boldsymbol{S}_i}^2 \tag{10a}$$

$$s.t.\ \tilde{\boldsymbol{y}}(k+1)=\tilde{\boldsymbol{y}}_0(k+1)+\boldsymbol{G}\Delta\boldsymbol{u}_M(k) \tag{10b}$$

$$\boldsymbol{y}_{\mathrm{LL}}-\boldsymbol{\varepsilon}(k+i)\le\tilde{\boldsymbol{y}}(k+i)\le\boldsymbol{y}_{\mathrm{HL}}+\boldsymbol{\varepsilon}(k+i)\quad i=1,\cdots,P \tag{10c}$$

$$\boldsymbol{u}_{\mathrm{LL}}\le\boldsymbol{u}(k+i)\le\boldsymbol{u}_{\mathrm{HL}}\quad i=0,\cdots,M-1 \tag{10d}$$

$$\Delta\boldsymbol{u}_{\mathrm{LL}}\le\Delta\boldsymbol{u}(k+i)\le\Delta\boldsymbol{u}_{\mathrm{HL}}\quad i=0,\cdots,M-1 \tag{10e}$$

$$-\boldsymbol{\varepsilon}(k+i)\le 0\quad i=1,\cdots,P \tag{10f}$$

Here, to drive the process variables to their optimal steady-state targets calculated by SSTC, the dynamic objective function is modified as

$$\min_{\substack{\Delta\boldsymbol{u}(k),\cdots,\Delta\boldsymbol{u}(k+M-1)\\ \boldsymbol{\varepsilon}(k),\cdots,\boldsymbol{\varepsilon}(k)}} \sum_{i=1}^{P}\left\|\boldsymbol{y}_{\mathrm{SS}}^*(k)-\tilde{\boldsymbol{y}}(k+i)\right\|_{\boldsymbol{Q}_i}^2 + \sum_{i=1}^{M}\left\|\boldsymbol{u}_{\mathrm{SS}}^*(k)-\boldsymbol{u}(k+i)\right\|_{\boldsymbol{V}_i}^2 + \sum_{i=1}^{M}\|\Delta\boldsymbol{u}(k+i)\|_{\boldsymbol{R}_i}^2+\sum_{i=1}^{P}\|\boldsymbol{\varepsilon}(k+i)\|_{\boldsymbol{S}_i}^2 \tag{11a}$$

$$s.t.\ \tilde{\boldsymbol{y}}_{PM}(k+1)=\tilde{\boldsymbol{y}}_{P0}(k+1)+\boldsymbol{A}\Delta\boldsymbol{u}_M(k) \tag{11b}$$

$$\boldsymbol{y}_{\mathrm{LL}}-\boldsymbol{\varepsilon}(k+i)\le\tilde{\boldsymbol{y}}(k+i|k)\le\boldsymbol{y}_{\mathrm{HL}}+\boldsymbol{\varepsilon}(k+i)\quad i=1,\cdots,P \tag{11c}$$

$$\boldsymbol{u}_{\mathrm{LL}}\le\boldsymbol{u}(k+i)\le\boldsymbol{u}_{\mathrm{HL}}\quad i=0,\cdots,M-1 \tag{11d}$$

$$\Delta\boldsymbol{u}_{\mathrm{LL}}\le\Delta\boldsymbol{u}(k+i)\le\Delta\boldsymbol{u}_{\mathrm{HL}}\quad i=0,\cdots,M-1 \tag{11e}$$

$$-\boldsymbol{\varepsilon}(k+i)\le 0\quad i=1,\cdots,P \tag{11f}$$

where the objective function in (11a) involves four penalty terms: future output deviations from the optimal steady-state output $\boldsymbol{y}_{\mathrm{SS}}^*$, future input deviations from the optimal steady-state input $\boldsymbol{u}_{\mathrm{SS}}^*$, control movements $\Delta\boldsymbol{u}$ and output constraint violations; Equation (11b) is the melting process model constraint; and four inequality constraints: input constraints (11c), output constraints (11d), control movement constraints (11e) and output constraint slack variable constraints (11f) are considered.

IV. INDUSTRIAL APPLICATION

The application of the proposed algorithm is based on F1 furnace with 90 ton/batch in Tianjin, China. Maintaining the original hardware equipment, a host computer named "APC Server" which communicates with Siemens PLC via TCP/IP is installed. The main components are illustrated in Figure 1. The architecture of F1 furnace control system is shown in Figure 3.

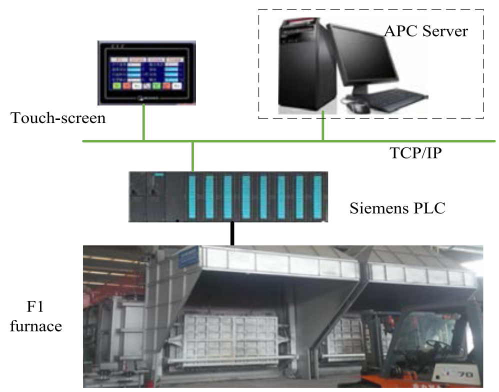

FIGURE 3. Architecture of F1 furnace control system.

A. SIMULATION OF ALUMINUM MELTING PROCESS FOR F1 FURNACE

Next, a simulation of the aluminum melting process analyzes the main factors. Since the aluminum melting is a complex reaction process with multiphase and multicomponent, Aspen Plus process simulation software is used to reduce the workload of process simulation, and the following assumptions are made:

1) Assume that the melting process was a continuous process, and the feeding speed the same as the discharging speed which was 6 ton/h.
2) Neglect the radiative heat transfer of inner surface of furnace.
3) The heat loss of furnace wall relies mainly on convective heat transfer.
4) One step fast non-reversible chemical reaction is adopted in combustion.
5) Alloy elements are surrounded completely by liquid aluminum.
6) Ignore the flow of liquid aluminum caused by temperature difference.

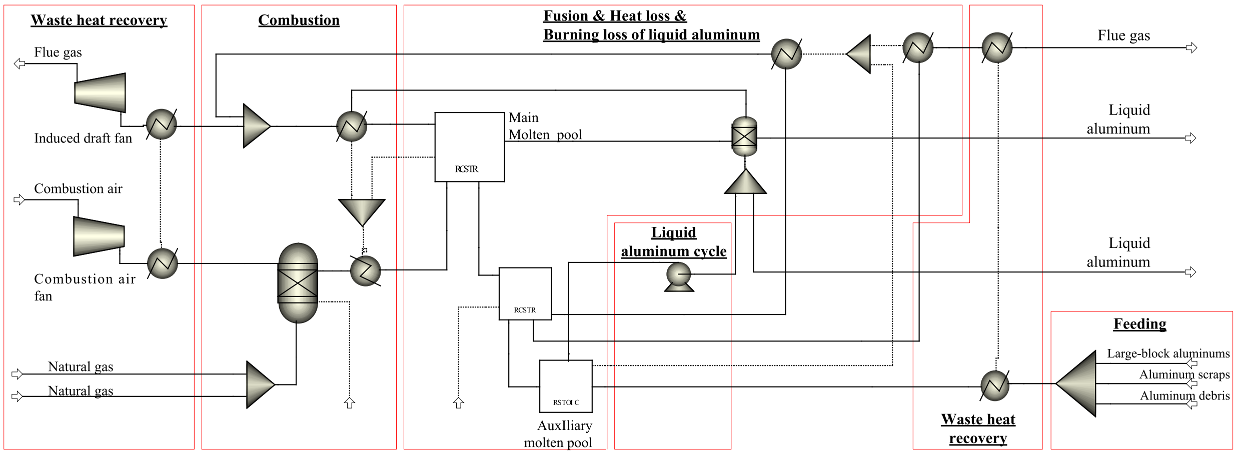

FIGURE 4. Diagram of a melting process simulation for F1 furnace in Aspen Plus.

TABLE 1. Operating points for F1 furnace.

Description	Average operating points			Unit
	Optimization	Present	Original	
Comprehensive energy consumption E	8424427.71	9046327.83	9623112.72	kJ/h
Comprehensive energy consumption for unit output of product e_p	1420.57	1535.66	1643.47	kJ/kg·h
Power consumption of induced draft fan	22180.88	24750.01	23580.00	W
Power consumption of combustion air fan	9649.04	11895.22	7715.20	W
Total Al2O3 output	131.65	206.20	273.20	kg/h
Consumption of natural gas	234.08	251.11	267.90	m^3/h
Temperature of liquid aluminum	715.50	720.60	740.90	°C
Temperature of furnace chamber	972.46	1002.00	1035.00	°C
Furnace pressure	-10.00	-8.80	23.00	Pa
Temperature of aluminum scraps	175.62	170.25	133.54	°C
Temperature of flue gas	120.00	134.75	99.10	°C
oxygen content in flue gas	2.00	8.10	11.00	%

In terms of the structure of F1 furnace, the following sub-processes are considered to simulate the smelting process:

1) Waste heat recovery sub-process: heat storage medium and solid aluminum material are preheated by flue gas in this sub-process.
2) Combustion sub-process: the combustion reaction of natural gas is thought to be a simple and fast chemical reaction, that is, the combustion reaction is always in equilibrium. The degree and rate of combustion reaction will be determined based on the Gibbs principle of minimum free energy.
3) Fusion sub-process: the total heat required for melting one mole of aluminum is calculated by the following formula:

$$Q = \Delta H_s + \Delta H_M + \Delta H_l \tag{12}$$

where Q is the total theoretical heat, J/mol; ΔH_s and ΔH_l are the solid and liquid aluminum enthalpy respectively, J/mol; ΔH_M is the latent heat of fusion of aluminum, J/mol;

4) Burning loss of liquid aluminum sub-process: the burning loss of liquid aluminum is mainly caused by volatilization and chemical reaction.
5) Liquid aluminum cycle sub-process: the liquid aluminum in the main molten pool and the auxiliary molten pool is circulated through a circulating pump.
6) Heat loss sub-process: the radiating heat loss of furnace wall in melting process is mainly considered.
7) Feeding sub-process: large-block aluminums, aluminum debris and aluminum scraps are included.

The simulation of melting process is established through Aspen Plus as shown in Figure 4. Considering the processing capacity of the F1 furnace with the objective function of minimizing energy and material consumption, the optimal operating points are calculated as shown in Table 1.

Note that the reduction of total Al_2O_3 output indicates that the burning loss of liquid aluminum is down and the production of liquid aluminum is up. The increase of power consumption of induced draft fan illustrates that the utilization of waste heat is improved. The increase of power consumption of combustion air fan and the reduction of consumption of natural gas mean the combustion of natural gas more completely. Taking Chinese standard GB/T 2589-2008 [24] as a reference, lower heating value (LHV) of natural gas and electricity are 35500 kJ/ m^3 and 3600 kJ/(kW·h) respectively. Comparing to on-off controller, the integration of numerical simulation and control scheme proposed in this paper reduces the comprehensive energy consumption E 12.46%, and the comprehensive energy consumption for unit output of product e_p 13.56%.

B. TWO-LAYER MPC

Even with the MPC using a centralized model, which has a better performance than decentralized control, this advantage is based on a sufficient accurate model. In addition, designing, tuning and maintaining a centralized controller are extremely difficult [18], [25]. On the other hand, ignoring the interactions in controller design can lead to poor control performance or even instability. Here, another solution with a partially decentralized model is adopted to simplify the implementation of MPC for F1 furnace. Although the control movements calculated by MPC with a partially decentralized model structure is not optimal, the implementation of MPC is simplified and the robustness of the control system is improved. Pairing manipulated variables and controlled variables for structuring a partially decentralized model is important for minimizing interactions. Here, a criterion based on relative normalized gain array (RNGA) [26]–[28] is introduced to determine the partially decentralized model structure of MPC for F1 furnace. The lists of manipulated variables, controlled variables and disturbance variables in the two-layer MPC are shown in Table 2-4, and the priorities of the controlled variable constraints classified into three types: safety constraints, quality constraints and economic constraints ordered from high to low are shown in Table 5.

TABLE 2. Manipulated variables.

Variable	Tag	Unit	Description
u_1	FIC-001	%	openness of the natural gas valve
u_2	FIC-002	Hz	Running frequency of the combustion air fan
u_3	FIC-003	Hz	Running frequency of the induced draft fan

TABLE 3. Controlled variables.

Variable	Tag	Unit	Description
y_1	TIC-001	°C	Temperature of furnace chamber
y_2	TI-005	°C	Temperature of liquid aluminum
y_3	TI-007	°C	Temperature of aluminum scraps
y_4	AI-001	%	Oxygen content in flue gas
y_5	RI-001	%	Air-fuel ratios
y_6	PI-001	Pa	Furnace pressure
y_7	TI-008	°C	Temperature of flue gas: (TI-010 + TI-011) / 2

The partially decentralized model structure for MPC is shown as Figure 5, where the open-loop transfer function of each sub-model is described as a first-order plus dead time (FOPDT) form.

As can be seen from the decentralized model structure and control objective mentioned above, the control scheme of F1 furnace includes:

TABLE 4. Disturbance variables.

Variable	Tag	Unit	Description
f_1	FI-002	Nm^3/h	combustion air flow

TABLE 5. Priorities of the controlled variable constraints.

Priority	Constraint	Priority	Constraint
1	PI-001_HL PI-001_LL	5	TI-005_LL
2	TI-008_HL TI-008_LL TI-007_HL	6	RI-001_HL RI-001_LL
3	TI-001_HL TI-001_LL	7	AI-001_HL AI-001_LL
4	TI-005_HL	8	TI-007_LL

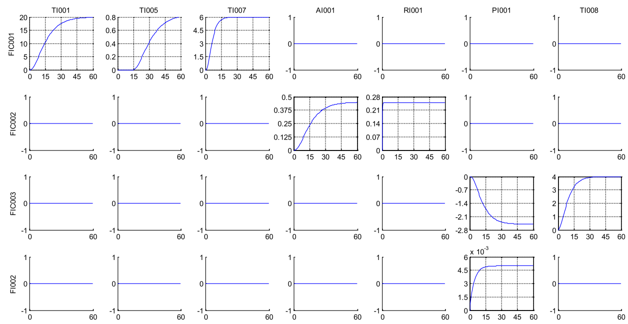

FIGURE 5. Partially decentralized model structure of F1 furnace.

1) SUSTAINED PRODUCTION SAFETY

The furnace press is controlled by using the running frequency of the induced draft fan as a manipulated variable and combustion air flow as a disturbance variable. This control loop compensates the furnace press fluctuation caused by combustion air flow, which ensures the furnace pressure is safe.

The temperature of flue gas is controlled by using the running frequency of the induced draft fan as a manipulated variable. This control loop aims to drive the temperature of flue gas to its optimal steady-state obtained from SSTC, which is helpful to improve energy utilization and ensure the safety of F1 furnace for that high temperature of flue gas will melt aluminum debris and aluminum scraps fed from rotary kilns and low temperature will corrode the chimney.

2) PROVISIONING ON-DEMAND

To minimize the usage amount of natural gas, the optimal steady-state of openness of the natural gas valve, temperature of furnace chamber, temperature of liquid aluminum and temperature of aluminum scraps are calculated by SSTC. In DO, these variables are controlled by openness of the natural gas valve as a manipulated variable. Due to predictive ability of MPC, when the temperature of liquid aluminum is close to its optimal steady-state, openness of the natural gas valve will be reduced in advance to avoid the temperature of liquid aluminum overshoot. Burning loss of liquid aluminum is avoided and provisioning on-demand of natural gas is achieved.

3) COMBUSTION EFFICIENCY OPTIMIZATION

Oxygen content in flue gas is an important index to detect combustion efficiency. Due to the hysteresis of physical instrument detection, Air-fuel ratio (combustion air flow/natural gas flow) is introduced as the auxiliary controlled variable. The oxygen content in fuel gas and the air-fuel ratio is controlled by using the running frequency of the combustion air fan as a manipulated variable. This control loop is used to ensure the optimum ratio of fuel and air in the melting process of F1 furnace and achieve combustion efficiency optimization.

C. APPLICATION RESULTS AND DISCUSSION

An on-off controller was adopted for F1 furnace previously. The manipulated variables were openness of the natural gas valve, running frequency of the combustion air fan and running frequency of the induced draft fan. Each of these manipulated variables had two constant states, high fire state and low fire state. There were two control modes for operators to choose by the switch button on the touch panel, the furnace chamber temperature control mode and the liquid aluminum temperature control mode. The controlled variable was furnace chamber temperature for the furnace chamber temperature control mode, and liquid aluminum temperature for the liquid aluminum temperature control mode.

In order to reduce the fluctuations of controlled variables caused by large time delays, the setting of thresholds was added for the two control modes as shown in Figure 6.

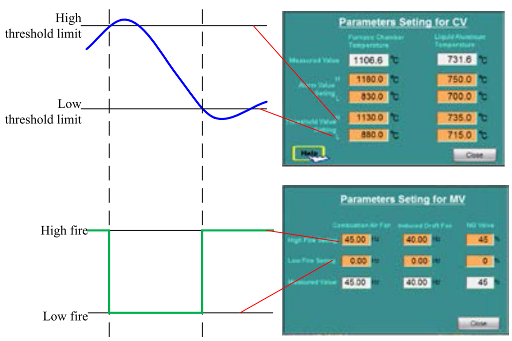

FIGURE 6. The operation interface of parameters setting for on-off controller.

For the furnace chamber temperature control mode, trends of the process variables under the on-off controller are depicted in Figure 7.

It can be seen in Figure 7 that at the sampling time 61 and 273, the furnace chamber temperature is greater than the upper limit, then openness of the natural gas valve (0%), running frequency of the combustion air fan (0Hz) and running frequency of the induced draft fan (0Hz) are switched to low fire states. at the sampling time 137 and 289, the furnace chamber temperature exceeds the lower limit, then openness of the natural gas valve (45%), running frequency of the combustion air fan (45Hz) and running frequency of the

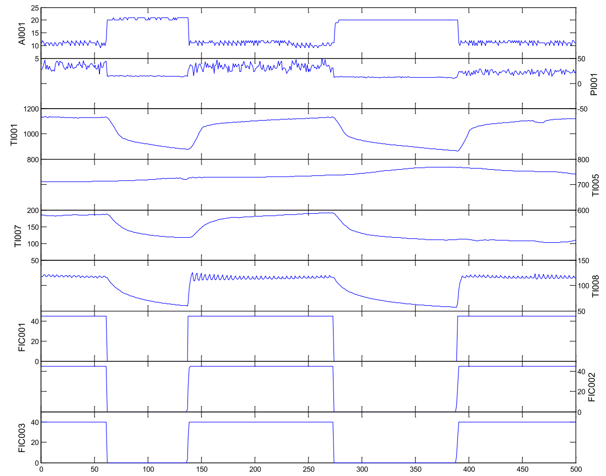

FIGURE 7. Control effect of F1 furnace with on-off control.

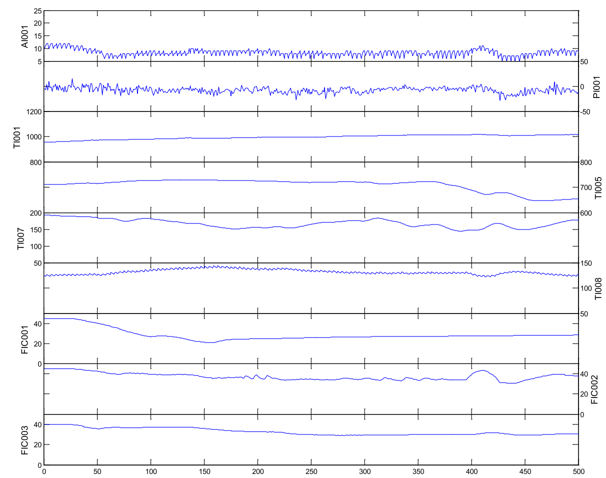

FIGURE 8. Control effect of F1 furnace with energy conservation oriented two-layer MPC.

induced draft fan (40Hz) are switched to high fire states. As a result of the switch action, the controlled variables will be constantly fluctuating with large amplitudes, some variables such as temperature of furnace chamber, temperature of flue gas and temperature of aluminum scraps even beyond their safety limits, which brings risks to safety production. In addition, the mean value of oxygen content in flue gas has been maintained at a high level about 11%.

The curves after the application of energy conservation oriented two-layer MPC are shown as Figure 8, in which from the sampling time 370 to 430, the furnace door is opened for adding large-block solid aluminums. As shown in Figure 8, the mean values of manipulated variables are reduced compared to these in the original control system used an on-off controller. particularly, the reduction of the natural gas valve openness is the most obvious. Before adding large-block solid aluminums, the temperature of liquid aluminum is kept around 720 °C, which is about 20 °C less than that in Figure 8. The lower temperature of liquid aluminum can not only help to reduce the consumption of natural gas, but also to increase production of products by reducing burning loss. After adding large-block solid aluminums, the temperature of furnace chamber is maintained at its upper limit to heat aluminum material quickly and ensure liquid aluminum without burning loss. However, due to the characteristics of aluminum, the temperature of liquid aluminum liquid rises slowly. The fluctuating of the aluminum scraps temperature is significantly reduced, and the mean value is about 170 °C which is increased by 30 °C comparing with the original system. The temperature of flue gas is always in the safety zone, and the men value is about 134 °C, which reduces the heat loss in the case of safety. Due to adopting multipriority-based SSTC for constraints relaxation, the economic goals with low priority can be achieved. As can be seen from Figure 8, the oxygen content in flue gas, the key factor to represent the combustion efficiency, always is maintained around 8% improved by 3%. Due to reasons such as flue air leakage and model mismatch, there is still a certain gap with the optimal steady-state. Taking GB/T 2589-2008 [24] as a reference in the same way, the comprehensive energy consumption E_{MPC} and the comprehensive energy consumption for unit output of product $e_{p,MPC}$ are 9046327.83 kJ/h and 1535.66 kJ/(kg · h) respectively, which decrease 5.99% and 6.56%.

According to the above analysis, it can be concluded that, after the application of energy conservation oriented two-layer MPC for F1 furnace, the combustion efficiency is improved effectively, and the energy consumption of the melting process is reduced.

V. CONCLUSION

In this paper, it has been proposed an energy conservation oriented two-layer MPC, in which direct measures and indirect measures are taken into consideration simultaneously. Multi-priority constraints relaxation based on safety, quality and energy efficiency is adopted to make steady-state target of SSTC feasible and reasonable, and a partially decentralized model structure is introduced to improve the robustness of the system. Through the simulation of F1 furnace, some operational recommendations are proposed. An energy conservation oriented two-layer MPC controller for F1 furnace is set up to achieve control objectives, including sustained production safety, provisioning on-demand and combustion efficiency optimization. By compared with the original on-off controller, application results demonstrate that the operation of F1 furnace is smoothly and the average of variables representing energy consumption, such as the openness of the natural gas valve, temperature of flue gas and oxygen content in flue gas, are significantly reduced. The comprehensive energy consumption and the comprehensive energy consumption for unit output of product respectively decrease 5.99% and 6.56% compared to operation under the previous on-off controller.

Future works include the study of online nonlinear steady-state optimization and a linear parameter varying model to improve the accuracy of F1 furnace model.

REFERENCES

[1] Z. Yang, S. Shao, L. Yang, and J. Liu, "Differentiated effects of diversified technological sources on energy-saving technological progress: Empirical evidence from China's industrial sectors," *Renew. Sustain. Energy Rev.*, vol. 72, pp. 1379–1388, May 2017.

[2] L. Acevedo, S. Usón, and J. Uche, "Exergy transfer analysis of an aluminum holding furnace," *Energy Convers. Manage.*, vol. 89, pp. 484–496, Jan. 2015.

[3] P. Royo, V. J. Ferreira, A. M. López-Sabirón, T. García-Armingol, and G. Ferreira, "Retrofitting strategies for improving the energy and environmental efficiency in industrial furnaces: A case study in the aluminium sector," *Renew. Sustain. Energy Rev.*, vol. 82, pp. 1813–1822, Feb. 2018.

[4] C. Belt, "Current state of aluminum melting and holding furnaces in industry," *Proc. JOM*, vol. 67, no. 11, pp. 2690–2695, Nov. 2015.

[5] K. He and L. Wang, "A review of energy use and energy-efficient technologies for the iron and steel industry," *Renew. Sustain. Energy Rev.*, vol. 70, pp. 1022–1039, Apr. 2017.

[6] A. Jakovics, I. Madzhulis, V. Frishfelds, and B. Nacke, "Influence of melt flow and temperature on erosion of refractory and deposit formation in aluminium melting furnaces," *Energy Convers. Manage.*, vol. 43, no. 3, pp. 345–352, Feb. 2002.

[7] F. Dal Magro, A. Meneghetti, G. Nardin, and S. Savino, "Enhancing energy recovery in the steel industry: Matching continuous charge with off-gas variability smoothing," *Energy Convers. Manage.*, vol. 104, pp. 78–89, Nov. 2015.

[8] A. O. Nieckele, M. F. Naccache, and M. S. P. Gomes, "Combustion performance of an aluminum melting furnace operating with natural gas and liquid fuel," *Appl. Thermal Eng.*, vol. 31, no. 5, pp. 841–851, Apr. 2011.

[9] J.-M. Wang, H.-J. Yan, J.-M. Zhou, S.-X. Li, and G.-C. Gui, "Optimization of parameters for an aluminum melting furnace using the Taguchi approach," *Appl. Thermal Eng.*, vols. 33–34, pp. 33–34, Feb. 2012.

[10] K. J. Åström and P. R. Kumar, "Control: A perspective," *Automatica*, vol. 50, no. 1, pp. 3–43, 2014.

[11] Z. Palmor, "Stability properties of Smith dead-time compensator controllers," *Int. J. Control*, vol. 32, no. 6, pp. 937–949, May 1980.

[12] R. Sanz, P. P. García, and P. Albertos, "A generalized smith predictor for unstable time-delay SISO systems," *ISA Trans.*, vol. 72, pp. 197–204, Jan. 2018.

[13] M. Beschi, A. Visioli, M. Berenguel, and L. J. Yebra, "Constrained temperature control of a solar furnace," *IEEE Trans. Control Syst. Technol.*, vol. 20, no. 5, pp. 1263–1274, Sep. 2012.

[14] J. Peng, H. He, and R. Xiong, "Rule based energy management strategy for a series–parallel plug-in hybrid electric bus optimized by dynamic programming," *Appl. Energy*, vol. 185, pp. 1633–1643, Jan. 2017.

[15] R. D. Martín, F. Obeso, J. Mochón, R. Barea, and J. Jiménez, "Hot metal temperature prediction in blast furnace using advanced model based on fuzzy logic tools," *Ironmaking Steelmaking*, vol. 34, no. 3, pp. 241–247, Jul. 2013.

[16] Z. Wu, T. Liu, Z.-P. Jiang, T. Chai, and L. Zhang, "Nonlinear control tools for fused magnesium furnaces: Design and implementation," *IEEE Trans. Ind. Electron.*, vol. 65, no. 9, pp. 7248–7257, Sep. 2108.

[17] S. J. Qin and T. A. Badgwell, "A survey of industrial model predictive control technology," *Control Eng. Pract.*, vol. 11, no. 7, pp. 733–764, 2003.

[18] D. Q. Mayne, "Model predictive control: Recent developments and future promise," *Automatica*, vol. 50, no. 12, pp. 2967–2986, 2014.

[19] A. Grancharova, J. Kocijan, and T. A. Johansen, "Explicit stochastic predictive control of combustion plants based on Gaussian process models," *Automatica*, vol. 44, no. 6, pp. 1621–1631, 2008.

[20] R. Zhang, Q. Zou, Z. Cao, and F. Gao, "Design of fractional order modeling based extended non-minimal state space MPC for temperature in an industrial electric heating furnace," *J. Process Control*, vol. 56, pp. 13–22, Aug. 2017.

[21] H. S. Ganesh, T. F. Edgar, and M. Baldea, "Model predictive control of the exit part temperature for an austenitization furnace," *Processes*, vol. 4, no. 4, pp. 53–66, Dec. 2016.

[22] S. Banerjee, D. Sanyal, S. Sen, and I. K. Puri, "A methodology to control direct-fired furnaces," *Int. J. Heat Mass Transf.*, vol. 47, no. 24, pp. 5247–5256, Nov. 2004.

[23] V. Havlena and J. Findejs, "Application of model predictive control to advanced combustion control," *Control Eng. Pract.*, vol. 13, no. 6, pp. 671–680, Jun. 2005.

[24] *General Principles for Calculation of the Comprehensive Energy Consumption*, document GB/T2589-2008, 2008.

[25] R. Scattolini, "Architectures for distributed and hierarchical model predictive control—A review," *J. Process Control*, vol. 19, no. 5, pp. 723–731, May 2009.
[26] S. Skogestad, "Plantwide control: The search for the self-optimizing control structure," *J. Process Control*, vol. 10, no. 5, pp. 487–507, Oct. 2000.
[27] S. Skogestad, "Control structure design for complete chemical plants," *Comput. Chem. Eng.*, vol. 28, nos. 1–2, pp. 219–234, Jan. 2004.
[28] D. Jolevski, O. Bego, and P. Sarajcev, "Control structure design and dynamics modelling of the organic Rankine cycle system," *Energy*, vol. 121, pp. 193–204, Feb. 2017.

NA GUO was born in Dingzhou, Hebei, China, in 1983. She received the Ph.D. degree in mechatronic engineering from the Shenyang Institute of Automation (SIA), Chinese Academy of Sciences, Shenyang, China, in 2015. Since 2015, she has been a Teacher with the College of Engineering, Shenyang Agricultural University. Her research interests include advanced process control and agricultural intelligent control.

HONGYU ZHENG received the B.S. degree in automation and the M.S. degree in control theory and control engineering from the Shenyang University of Chemical Technology, Shenyang, China, in 2008 and 2011, respectively, and the Ph.D. degree in detection technology and automatic equipment from Northeastern University, Shenyang, in 2019. Since March 2019, he has been a Teacher with the School of Intelligent Manufacturing, Huanghuai University. His research interests include advanced process control and optimization.

TAO ZOU was born in Dashiqiao, Liaoning, China, in 1975. He received the Ph.D. degree in control theory and control engineering from Shanghai Jiao Tong University, Shanghai, China, in 2005. Since 2017, he has been a Researcher with the Shenyang Institute of Automation (SIA), Chinese Academy of Sciences. His research interests include industrial process modeling and simulation, model predictive control, advanced process control, and real-time optimization technology research and application.

YANG JIA was born in Dashiqiao, Liaoning, China, in 1984. He received the B.S. degree in chemical engineering and the M.S. degree in chemical engineering from the Dalian University of Technology, Dalian, China, in 2008 and 2011, respectively. Since 2013, he has been an Associate Researcher with the Shenyang Institute of Automation (SIA), Chinese Academy of Sciences. His research interests include industrial process modeling and simulation, operation optimization, and energy utilization.